

Observation of $e^+e^- \rightarrow \rho^+\rho^-$ near $\sqrt{s} = 10.58$ GeV

B. Aubert,¹ M. Bona,¹ Y. Karyotakis,¹ J. P. Lees,¹ V. Poireau,¹ E. Prencipe,¹ X. Prudent,¹ V. Tisserand,¹
J. Garra Tico,² E. Grauges,² L. Lopez^{ab,3}, A. Palano^{ab,3}, M. Pappagallo^{ab,3}, G. Eigen,⁴ B. Stugu,⁴ L. Sun,⁴
G. S. Abrams,⁵ M. Battaglia,⁵ D. N. Brown,⁵ R. N. Cahn,⁵ R. G. Jacobsen,⁵ L. T. Kerth,⁵ Yu. G. Kolomoisky,⁵
G. Kukartsev,⁵ G. Lynch,⁵ I. L. Osipenkov,⁵ M. T. Ronan,^{5,*} K. Tackmann,⁵ T. Tanabe,⁵ C. M. Hawkes,⁶
N. Soni,⁶ A. T. Watson,⁶ H. Koch,⁷ T. Schroeder,⁷ D. Walker,⁸ D. J. Asgeirsson,⁹ B. G. Fulsom,⁹
C. Hearty,⁹ T. S. Mattison,⁹ J. A. McKenna,⁹ M. Barrett,¹⁰ A. Khan,¹⁰ L. Teodorescu,¹⁰ V. E. Blinov,¹¹
A. D. Bukin,¹¹ A. R. Buzykaev,¹¹ V. P. Druzhinin,¹¹ V. B. Golubev,¹¹ A. P. Onuchin,¹¹ S. I. Serednyakov,¹¹
Yu. I. Skovpen,¹¹ E. P. Solodov,¹¹ K. Yu. Todyshev,¹¹ M. Bondioli,¹² S. Curry,¹² I. Eschrich,¹² D. Kirkby,¹²
A. J. Lankford,¹² P. Lund,¹² M. Mandelkern,¹² E. C. Martin,¹² D. P. Stoker,¹² S. Abachi,¹³ C. Buchanan,¹³
J. W. Gary,¹⁴ F. Liu,¹⁴ O. Long,¹⁴ B. C. Shen,^{14,*} G. M. Vitug,¹⁴ Z. Yasin,¹⁴ L. Zhang,¹⁴ V. Sharma,¹⁵
C. Campagnari,¹⁶ T. M. Hong,¹⁶ D. Kovalskyi,¹⁶ M. A. Mazur,¹⁶ J. D. Richman,¹⁶ T. W. Beck,¹⁷ A. M. Eisner,¹⁷
C. J. Flacco,¹⁷ C. A. Heusch,¹⁷ J. Kroseberg,¹⁷ W. S. Lockman,¹⁷ T. Schalk,¹⁷ B. A. Schumm,¹⁷ A. Seiden,¹⁷
L. Wang,¹⁷ M. G. Wilson,¹⁷ L. O. Winstrom,¹⁷ C. H. Cheng,¹⁸ D. A. Doll,¹⁸ B. Echenard,¹⁸ F. Fang,¹⁸
D. G. Hitlin,¹⁸ I. Narsky,¹⁸ T. Piatenko,¹⁸ F. C. Porter,¹⁸ R. Andreassen,¹⁹ G. Mancinelli,¹⁹ B. T. Meadows,¹⁹
K. Mishra,¹⁹ M. D. Sokoloff,¹⁹ P. C. Bloom,²⁰ W. T. Ford,²⁰ A. Gaz,²⁰ J. F. Hirschauer,²⁰ A. Kreisel,²⁰
M. Nagel,²⁰ U. Nauenberg,²⁰ J. G. Smith,²⁰ K. A. Ulmer,²⁰ S. R. Wagner,²⁰ R. Ayad,^{21,†} A. Soffer,^{21,‡}
W. H. Toki,²¹ R. J. Wilson,²¹ D. D. Altenburg,²² E. Feltresi,²² A. Hauke,²² H. Jasper,²² M. Karbach,²² J. Merkel,²²
A. Petzold,²² B. Spaan,²² K. Wacker,²² M. J. Kobel,²³ W. F. Mader,²³ R. Nogowski,²³ K. R. Schubert,²³
R. Schwierz,²³ J. E. Sundermann,²³ A. Volk,²³ D. Bernard,²⁴ G. R. Bonneaud,²⁴ E. Latour,²⁴ Ch. Thiebaux,²⁴
M. Verderi,²⁴ P. J. Clark,²⁵ W. Gradl,²⁵ S. Playfer,²⁵ J. E. Watson,²⁵ M. Andreotti^{ab,26}, D. Bettoni^{a,26}, C. Bozzi^{a,26},
R. Calabrese^{ab,26}, A. Cecchi^{ab,26}, G. Cibinetto^{ab,26}, P. Franchini^{ab,26}, E. Luppi^{ab,26}, M. Negrini^{ab,26}, A. Petrella^{ab,26},
L. Piemontese^{a,26}, V. Santoro^{ab,26}, R. Baldini-Ferrolli,²⁷ A. Calcaterra,²⁷ R. de Sangro,²⁷ G. Finocchiaro,²⁷
S. Pacetti,²⁷ P. Patteri,²⁷ I. M. Peruzzi,^{27,§} M. Piccolo,²⁷ M. Rama,²⁷ A. Zallo,²⁷ A. Buzzo^{a,28}, R. Contri^{ab,28},
M. Lo Vetere^{ab,28}, M. M. Macri^{a,28}, M. R. Monge^{ab,28}, S. Passaggio^{a,28}, C. Patrignani^{ab,28}, E. Robutti^{a,28},
A. Santroni^{ab,28}, S. Tosi^{ab,28}, K. S. Chaisanguanthum,²⁹ M. Morii,²⁹ J. Marks,³⁰ S. Schenk,³⁰ U. Uwer,³⁰
V. Klose,³¹ H. M. Lacker,³¹ D. J. Bard,³² P. D. Dauncey,³² J. A. Nash,³² W. Panduro Vazquez,³² M. Tibbetts,³²
P. K. Behera,³³ X. Chai,³³ M. J. Charles,³³ U. Mallik,³³ J. Cochran,³⁴ H. B. Crawley,³⁴ L. Dong,³⁴ W. T. Meyer,³⁴
S. Prell,³⁴ E. I. Rosenberg,³⁴ A. E. Rubin,³⁴ Y. Y. Gao,³⁵ A. V. Gritsan,³⁵ Z. J. Guo,³⁵ C. K. Lae,³⁵ A. G. Denig,³⁶
M. Fritsch,³⁶ G. Schott,³⁶ N. Arnaud,³⁷ J. Béguilleux,³⁷ A. D’Orazio,³⁷ M. Davier,³⁷ J. Firmino da Costa,³⁷
G. Grosdidier,³⁷ A. Höcker,³⁷ V. Lepeltier,³⁷ F. Le Diberder,³⁷ A. M. Lutz,³⁷ S. Pruvot,³⁷ P. Roudeau,³⁷
M. H. Schune,³⁷ J. Serrano,³⁷ V. Sordini,^{37,¶} A. Stocchi,³⁷ G. Wormser,³⁷ D. J. Lange,³⁸ D. M. Wright,³⁸
I. Bingham,³⁹ J. P. Burke,³⁹ C. A. Chavez,³⁹ J. R. Fry,³⁹ E. Gabathuler,³⁹ R. Gamet,³⁹ D. E. Hutchcroft,³⁹
D. J. Payne,³⁹ C. Touramanis,³⁹ A. J. Bevan,⁴⁰ C. K. Clarke,⁴⁰ K. A. George,⁴⁰ F. Di Lodovico,⁴⁰ R. Sacco,⁴⁰
M. Sigamani,⁴⁰ G. Cowan,⁴¹ H. U. Flaecher,⁴¹ D. A. Hopkins,⁴¹ S. Paramesvaran,⁴¹ F. Salvatore,⁴¹ A. C. Wren,⁴¹
D. N. Brown,⁴² C. L. Davis,⁴² K. E. Alwyn,⁴³ D. S. Bailey,⁴³ R. J. Barlow,⁴³ Y. M. Chia,⁴³ C. L. Edgar,⁴³
G. D. Lafferty,⁴³ T. J. West,⁴³ J. I. Yi,⁴³ J. Anderson,⁴⁴ C. Chen,⁴⁴ A. Jawahery,⁴⁴ D. A. Roberts,⁴⁴ G. Simi,⁴⁴
J. M. Tuggle,⁴⁴ C. Dallapiccola,⁴⁵ X. Li,⁴⁵ E. Salvati,⁴⁵ S. Saremi,⁴⁵ R. Cowan,⁴⁶ D. Dujmic,⁴⁶ P. H. Fisher,⁴⁶
K. Koeneke,⁴⁶ G. Sciolla,⁴⁶ M. Spitznagel,⁴⁶ F. Taylor,⁴⁶ R. K. Yamamoto,⁴⁶ M. Zhao,⁴⁶ P. M. Patel,⁴⁷
S. H. Robertson,⁴⁷ A. Lazzaro^{ab,48}, V. Lombardo^{a,48}, F. Palombo^{ab,48}, J. M. Bauer,⁴⁹ L. Cremaldi,⁴⁹
V. Eschenburg,⁴⁹ R. Godang,^{49,**} R. Kroeger,⁴⁹ D. A. Sanders,⁴⁹ D. J. Summers,⁴⁹ H. W. Zhao,⁴⁹ M. Simard,⁵⁰
P. Taras,⁵⁰ F. B. Viaud,⁵⁰ H. Nicholson,⁵¹ G. De Nardo^{ab,52}, L. Lista^{a,52}, D. Monorchio^{ab,52}, G. Onorato^{ab,52},
C. Sciacca^{ab,52}, G. Raven,⁵³ H. L. Snoek,⁵³ C. P. Jessop,⁵⁴ K. J. Knoepfel,⁵⁴ J. M. LoSecco,⁵⁴ W. F. Wang,⁵⁴
G. Benelli,⁵⁵ L. A. Corwin,⁵⁵ K. Honscheid,⁵⁵ H. Kagan,⁵⁵ R. Kass,⁵⁵ J. P. Morris,⁵⁵ A. M. Rahimi,⁵⁵
J. J. Regensburger,⁵⁵ S. J. Sekula,⁵⁵ Q. K. Wong,⁵⁵ N. L. Blount,⁵⁶ J. Brau,⁵⁶ R. Frey,⁵⁶ O. Igonkina,⁵⁶
J. A. Kolb,⁵⁶ M. Lu,⁵⁶ R. Rahmat,⁵⁶ N. B. Sinev,⁵⁶ D. Strom,⁵⁶ J. Strube,⁵⁶ E. Torrence,⁵⁶ G. Castelli^{ab,57}

N. Gagliardi^{ab,57} M. Margoni^{ab,57} M. Morandin^{a,57} M. Posocco^{a,57} M. Rotondo^{a,57} F. Simonetto^{ab,57} R. Stroili^{ab,57}
 C. Voci^{ab,57} P. del Amo Sanchez,⁵⁸ E. Ben-Haim,⁵⁸ H. Briand,⁵⁸ G. Calderini,⁵⁸ J. Chauveau,⁵⁸ P. David,⁵⁸
 L. Del Buono,⁵⁸ O. Hamon,⁵⁸ Ph. Leruste,⁵⁸ J. Ocariz,⁵⁸ A. Perez,⁵⁸ J. Prendki,⁵⁸ L. Gladney,⁵⁹ M. Biasini^{ab,60}
 R. Covarelli^{ab,60} E. Manoni^{ab,60} C. Angelini^{ab,61} G. Batignani^{ab,61} S. Bettarini^{ab,61} M. Carpinelli^{ab,61}, ††
 A. Cervelli^{ab,61} F. Forti^{ab,61} M. A. Giorgi^{ab,61} A. Lusiani^{ac,61} G. Marchiori^{ab,61} M. Morganti^{ab,61} N. Neri^{ab,61}
 E. Paoloni^{ab,61} G. Rizzo^{ab,61} J. J. Walsh^{a,61} J. Biesiada,⁶² D. Lopes Pegna,⁶² C. Lu,⁶² J. Olsen,⁶² A. J. S. Smith,⁶²
 A. V. Telnov,⁶² F. Anulli^{a,63} E. Baracchini^{ab,63} G. Cavoto^{a,63} D. del Re^{ab,63} E. Di Marco^{ab,63} R. Faccini^{ab,63}
 F. Ferrarotto^{a,63} F. Ferroni^{ab,63} M. Gaspero^{ab,63} P. D. Jackson^{a,63} L. Li Gioi^{a,63} M. A. Mazzoni^{a,63} S. Morganti^{a,63}
 G. Piredda^{a,63} F. Polci^{ab,63} F. Renga^{ab,63} C. Voena^{a,63} M. Ebert,⁶⁴ T. Hartmann,⁶⁴ H. Schröder,⁶⁴ R. Waldi,⁶⁴
 T. Adye,⁶⁵ B. Franek,⁶⁵ E. O. Olaiya,⁶⁵ W. Roethel,⁶⁵ F. F. Wilson,⁶⁵ S. Emery,⁶⁶ M. Escalier,⁶⁶ L. Esteve,⁶⁶
 A. Gaidot,⁶⁶ S. F. Ganzhur,⁶⁶ G. Hamel de Monchenault,⁶⁶ W. Kozanecki,⁶⁶ G. Vasseur,⁶⁶ Ch. Yèche,⁶⁶
 M. Zito,⁶⁶ X. R. Chen,⁶⁷ H. Liu,⁶⁷ W. Park,⁶⁷ M. V. Purohit,⁶⁷ R. M. White,⁶⁷ J. R. Wilson,⁶⁷ M. T. Allen,⁶⁸
 D. Aston,⁶⁸ R. Bartoldus,⁶⁸ P. Bechtel,⁶⁸ J. F. Benitez,⁶⁸ R. Cenci,⁶⁸ J. P. Coleman,⁶⁸ M. R. Convery,⁶⁸
 J. C. Dingfelder,⁶⁸ J. Dorfan,⁶⁸ G. P. Dubois-Felsmann,⁶⁸ W. Dunwoodie,⁶⁸ R. C. Field,⁶⁸ A. M. Gabareen,⁶⁸
 S. J. Gowdy,⁶⁸ M. T. Graham,⁶⁸ P. Grenier,⁶⁸ C. Hast,⁶⁸ W. R. Innes,⁶⁸ J. Kaminski,⁶⁸ M. H. Kelsey,⁶⁸ H. Kim,⁶⁸
 P. Kim,⁶⁸ M. L. Kocian,⁶⁸ D. W. G. S. Leith,⁶⁸ S. Li,⁶⁸ B. Lindquist,⁶⁸ S. Luitz,⁶⁸ V. Luth,⁶⁸ H. L. Lynch,⁶⁸
 D. B. MacFarlane,⁶⁸ H. Marsiske,⁶⁸ R. Messner,⁶⁸ D. R. Muller,⁶⁸ H. Neal,⁶⁸ S. Nelson,⁶⁸ C. P. O'Grady,⁶⁸ I. Ofte,⁶⁸
 A. Perazzo,⁶⁸ M. Perl,⁶⁸ B. N. Ratcliff,⁶⁸ A. Roodman,⁶⁸ A. A. Salnikov,⁶⁸ R. H. Schindler,⁶⁸ J. Schwiening,⁶⁸
 A. Snyder,⁶⁸ D. Su,⁶⁸ M. K. Sullivan,⁶⁸ K. Suzuki,⁶⁸ S. K. Swain,⁶⁸ J. M. Thompson,⁶⁸ J. Va'vra,⁶⁸ A. P. Wagner,⁶⁸
 M. Weaver,⁶⁸ C. A. West,⁶⁸ W. J. Wisniewski,⁶⁸ M. Wittgen,⁶⁸ D. H. Wright,⁶⁸ H. W. Wulsin,⁶⁸ A. K. Yarritu,⁶⁸
 K. Yi,⁶⁸ C. C. Young,⁶⁸ V. Ziegler,⁶⁸ P. R. Burchat,⁶⁹ A. J. Edwards,⁶⁹ S. A. Majewski,⁶⁹ T. S. Miyashita,⁶⁹
 B. A. Petersen,⁶⁹ L. Wilden,⁶⁹ S. Ahmed,⁷⁰ M. S. Alam,⁷⁰ J. A. Ernst,⁷⁰ B. Pan,⁷⁰ M. A. Saeed,⁷⁰ S. B. Zain,⁷⁰
 S. M. Spanier,⁷¹ B. J. Wogslund,⁷¹ R. Eckmann,⁷² J. L. Ritchie,⁷² A. M. Ruland,⁷² C. J. Schilling,⁷²
 R. F. Schwitters,⁷² B. W. Drummond,⁷³ J. M. Izen,⁷³ X. C. Lou,⁷³ F. Bianchi^{ab,74} D. Gamba^{ab,74} M. Pelliccioni^{ab,74}
 M. Bomben^{ab,75} L. Bosisio^{ab,75} C. Cartaro^{ab,75} G. Della Ricca^{ab,75} L. Lanceri^{ab,75} L. Vitale^{ab,75} V. Azzolini,⁷⁶
 N. Lopez-March,⁷⁶ F. Martinez-Vidal,⁷⁶ D. A. Milanes,⁷⁶ A. Oyanguren,⁷⁶ J. Albert,⁷⁷ Sw. Banerjee,⁷⁷
 B. Bhuyan,⁷⁷ H. H. F. Choi,⁷⁷ K. Hamano,⁷⁷ R. Kowalewski,⁷⁷ M. J. Lewczuk,⁷⁷ I. M. Nugent,⁷⁷ J. M. Roney,⁷⁷
 R. J. Sobie,⁷⁷ T. J. Gershon,⁷⁸ P. F. Harrison,⁷⁸ J. Ilic,⁷⁸ T. E. Latham,⁷⁸ G. B. Mohanty,⁷⁸ H. R. Band,⁷⁹
 X. Chen,⁷⁹ S. Dasu,⁷⁹ K. T. Flood,⁷⁹ Y. Pan,⁷⁹ M. Pierini,⁷⁹ R. Prepost,⁷⁹ C. O. Vuosalo,⁷⁹ and S. L. Wu⁷⁹

(The BABAR Collaboration)

¹Laboratoire de Physique des Particules, IN2P3/CNRS et Université de Savoie, F-74941 Annecy-Le-Vieux, France

²Universitat de Barcelona, Facultat de Física, Departament ECM, E-08028 Barcelona, Spain

³INFN Sezione di Bari^a; Dipartimento di Fisica, Università di Bari^b, I-70126 Bari, Italy

⁴University of Bergen, Institute of Physics, N-5007 Bergen, Norway

⁵Lawrence Berkeley National Laboratory and University of California, Berkeley, California 94720, USA

⁶University of Birmingham, Birmingham, B15 2TT, United Kingdom

⁷Ruhr Universität Bochum, Institut für Experimentalphysik 1, D-44780 Bochum, Germany

⁸University of Bristol, Bristol BS8 1TL, United Kingdom

⁹University of British Columbia, Vancouver, British Columbia, Canada V6T 1Z1

¹⁰Brunel University, Uxbridge, Middlesex UB8 3PH, United Kingdom

¹¹Budker Institute of Nuclear Physics, Novosibirsk 630090, Russia

¹²University of California at Irvine, Irvine, California 92697, USA

¹³University of California at Los Angeles, Los Angeles, California 90024, USA

¹⁴University of California at Riverside, Riverside, California 92521, USA

¹⁵University of California at San Diego, La Jolla, California 92093, USA

¹⁶University of California at Santa Barbara, Santa Barbara, California 93106, USA

¹⁷University of California at Santa Cruz, Institute for Particle Physics, Santa Cruz, California 95064, USA

¹⁸California Institute of Technology, Pasadena, California 91125, USA

¹⁹University of Cincinnati, Cincinnati, Ohio 45221, USA

²⁰University of Colorado, Boulder, Colorado 80309, USA

²¹Colorado State University, Fort Collins, Colorado 80523, USA

²²Technische Universität Dortmund, Fakultät Physik, D-44221 Dortmund, Germany

²³Technische Universität Dresden, Institut für Kern- und Teilchenphysik, D-01062 Dresden, Germany

²⁴Laboratoire Leprince-Ringuet, CNRS/IN2P3, Ecole Polytechnique, F-91128 Palaiseau, France

²⁵University of Edinburgh, Edinburgh EH9 3JZ, United Kingdom

²⁶INFN Sezione di Ferrara^a; Dipartimento di Fisica, Università di Ferrara^b, I-44100 Ferrara, Italy

- ²⁷INFN Laboratori Nazionali di Frascati, I-00044 Frascati, Italy
- ²⁸INFN Sezione di Genova^a; Dipartimento di Fisica, Università di Genova^b, I-16146 Genova, Italy
- ²⁹Harvard University, Cambridge, Massachusetts 02138, USA
- ³⁰Universität Heidelberg, Physikalisches Institut, Philosophenweg 12, D-69120 Heidelberg, Germany
- ³¹Humboldt-Universität zu Berlin, Institut für Physik, Newtonstr. 15, D-12489 Berlin, Germany
- ³²Imperial College London, London, SW7 2AZ, United Kingdom
- ³³University of Iowa, Iowa City, Iowa 52242, USA
- ³⁴Iowa State University, Ames, Iowa 50011-3160, USA
- ³⁵Johns Hopkins University, Baltimore, Maryland 21218, USA
- ³⁶Universität Karlsruhe, Institut für Experimentelle Kernphysik, D-76021 Karlsruhe, Germany
- ³⁷Laboratoire de l'Accélérateur Linéaire, IN2P3/CNRS et Université Paris-Sud 11, Centre Scientifique d'Orsay, B. P. 34, F-91898 Orsay Cedex, France
- ³⁸Lawrence Livermore National Laboratory, Livermore, California 94550, USA
- ³⁹University of Liverpool, Liverpool L69 7ZE, United Kingdom
- ⁴⁰Queen Mary, University of London, London, E1 4NS, United Kingdom
- ⁴¹University of London, Royal Holloway and Bedford New College, Egham, Surrey TW20 0EX, United Kingdom
- ⁴²University of Louisville, Louisville, Kentucky 40292, USA
- ⁴³University of Manchester, Manchester M13 9PL, United Kingdom
- ⁴⁴University of Maryland, College Park, Maryland 20742, USA
- ⁴⁵University of Massachusetts, Amherst, Massachusetts 01003, USA
- ⁴⁶Massachusetts Institute of Technology, Laboratory for Nuclear Science, Cambridge, Massachusetts 02139, USA
- ⁴⁷McGill University, Montréal, Québec, Canada H3A 2T8
- ⁴⁸INFN Sezione di Milano^a; Dipartimento di Fisica, Università di Milano^b, I-20133 Milano, Italy
- ⁴⁹University of Mississippi, University, Mississippi 38677, USA
- ⁵⁰Université de Montréal, Physique des Particules, Montréal, Québec, Canada H3C 3J7
- ⁵¹Mount Holyoke College, South Hadley, Massachusetts 01075, USA
- ⁵²INFN Sezione di Napoli^a; Dipartimento di Scienze Fisiche, Università di Napoli Federico II^b, I-80126 Napoli, Italy
- ⁵³NIKHEF, National Institute for Nuclear Physics and High Energy Physics, NL-1009 DB Amsterdam, The Netherlands
- ⁵⁴University of Notre Dame, Notre Dame, Indiana 46556, USA
- ⁵⁵Ohio State University, Columbus, Ohio 43210, USA
- ⁵⁶University of Oregon, Eugene, Oregon 97403, USA
- ⁵⁷INFN Sezione di Padova^a; Dipartimento di Fisica, Università di Padova^b, I-35131 Padova, Italy
- ⁵⁸Laboratoire de Physique Nucléaire et de Hautes Energies, IN2P3/CNRS, Université Pierre et Marie Curie-Paris6, Université Denis Diderot-Paris7, F-75252 Paris, France
- ⁵⁹University of Pennsylvania, Philadelphia, Pennsylvania 19104, USA
- ⁶⁰INFN Sezione di Perugia^a; Dipartimento di Fisica, Università di Perugia^b, I-06100 Perugia, Italy
- ⁶¹INFN Sezione di Pisa^a; Dipartimento di Fisica, Università di Pisa^b; Scuola Normale Superiore di Pisa^c, I-56127 Pisa, Italy
- ⁶²Princeton University, Princeton, New Jersey 08544, USA
- ⁶³INFN Sezione di Roma^a; Dipartimento di Fisica, Università di Roma La Sapienza^b, I-00185 Roma, Italy
- ⁶⁴Universität Rostock, D-18051 Rostock, Germany
- ⁶⁵Rutherford Appleton Laboratory, Chilton, Didcot, Oxon, OX11 0QX, United Kingdom
- ⁶⁶DSM/Dapnia, CEA/Saclay, F-91191 Gif-sur-Yvette, France
- ⁶⁷University of South Carolina, Columbia, South Carolina 29208, USA
- ⁶⁸Stanford Linear Accelerator Center, Stanford, California 94309, USA
- ⁶⁹Stanford University, Stanford, California 94305-4060, USA
- ⁷⁰State University of New York, Albany, New York 12222, USA
- ⁷¹University of Tennessee, Knoxville, Tennessee 37996, USA
- ⁷²University of Texas at Austin, Austin, Texas 78712, USA
- ⁷³University of Texas at Dallas, Richardson, Texas 75083, USA
- ⁷⁴INFN Sezione di Torino^a; Dipartimento di Fisica Sperimentale, Università di Torino^b, I-10125 Torino, Italy
- ⁷⁵INFN Sezione di Trieste^a; Dipartimento di Fisica, Università di Trieste^b, I-34127 Trieste, Italy
- ⁷⁶IFIC, Universitat de Valencia-CSIC, E-46071 Valencia, Spain
- ⁷⁷University of Victoria, Victoria, British Columbia, Canada V8W 3P6
- ⁷⁸Department of Physics, University of Warwick, Coventry CV4 7AL, United Kingdom
- ⁷⁹University of Wisconsin, Madison, Wisconsin 53706, USA

(Dated: June 25, 2008)

We report the first observation of $e^+e^- \rightarrow \rho^+\rho^-$, in a data sample of 379 fb^{-1} collected with the BABAR detector at the PEP-II e^+e^- storage ring at center-of-mass energies near $\sqrt{s} = 10.58 \text{ GeV}$. We measure a cross section of $\sigma(e^+e^- \rightarrow \rho^+\rho^-) = 19.5 \pm 1.6(\text{stat}) \pm 3.2(\text{syst}) \text{ fb}$. Assuming production

through single-photon annihilation, there are three independent helicity amplitudes. We measure the ratios of their squared moduli to be $|F_{00}|^2 : |F_{10}|^2 : |F_{11}|^2 = 0.51 \pm 0.14(\text{stat}) \pm 0.07(\text{syst}) : 0.10 \pm 0.04(\text{stat}) \pm 0.01(\text{syst}) : 0.04 \pm 0.03(\text{stat}) \pm 0.01(\text{syst})$. The $|F_{00}|^2$ result is inconsistent with the prediction of 1.0 made by QCD models with a significance of 3.1 standard deviations including systematic uncertainties.

PACS numbers: 13.66.Bc, 13.25.-k, 14.40.Ev

The exclusive production of $J/\psi\eta_c$ and other double-charmonium vector-pseudoscalar (VP) pairs in e^+e^- collisions around the $\Upsilon(4S)$ mass ($\sqrt{s} \approx 10.58$ GeV) is observed [1, 2] at rates approximately ten times larger than the rates expected from QCD-based models [3]. Various theoretical efforts have been made to resolve the discrepancy [4]. Measurements of the process $e^+e^- \rightarrow \phi\eta$ [5] provide information on the $e^+e^- \rightarrow \text{VP}$ process in the strange quark sector. Study of the vector-vector (VV) process $e^+e^- \rightarrow \rho^+\rho^-$ can provide complementary information and test perturbative QCD at the amplitude level [6] through investigation of the VV angular distributions.

The charge-conjugation (C) even final states $\rho^0\rho^0$ and $\phi\rho^0$ are produced through e^+e^- two-virtual-photon annihilation (TVPA) [7–9]. For $\rho^+\rho^-$, C can be either positive or negative. However, due to the particles' charges, the $e^+e^- \rightarrow \rho^+\rho^-$ process is unlikely to occur via TVPA unless there is either significant final quark recombination between the products of the two virtual photons or final-state interactions (FSI) [10]. Assuming production through single-photon annihilation or $\Upsilon(4S)$ decay, the VV final state can be described with three independent helicity amplitudes. Any discrepancy between the amplitudes predicted by perturbative QCD and the experimental measurement might indicate contributions from mechanisms such as FSI. Such discrepancies could help to better understand the importance of FSI effects in $B \rightarrow VV$ decays [11].

This analysis uses 343 fb $^{-1}$ of e^+e^- data collected on the $\Upsilon(4S)$ resonance at 10.58 GeV and 36 fb $^{-1}$ collected 40 MeV below (off-resonance) with the *BABAR* detector at the SLAC PEP-II asymmetric-energy B factory. The *BABAR* detector is described in detail elsewhere [12]. Charged-particle momenta and energy loss are measured in the tracking system, which consists of a silicon vertex tracker (SVT) and a helium-isobutane drift chamber (DCH). Electrons and photons are detected in a CsI(Tl) calorimeter (EMC). Charged pion candidates are identified using likelihoods of specific ionization in the SVT and DCH, and of Cherenkov angle and photon counts measured in an internally reflecting ring-imaging Cherenkov detector. Photons are identified by clusters of energy deposited in the EMC that have shapes consistent with an electromagnetic shower. The clusters are required to be isolated, i.e., geometrically unassociated with charged tracks.

To form the $\rho^+\rho^-$ final state, we select events with ex-

actly two well-reconstructed oppositely-charged π^\pm and at least two well-reconstructed π^0 candidates. We require the π^\pm candidates to have at least 12 DCH hits and a laboratory polar angle well within the SVT acceptance of $0.41 < \theta < 2.54$ radians. The laboratory transverse momenta of the π^\pm candidates are required to be greater than 100 MeV/ c . The two charged tracks must both be identified as pions. We fit the two charged tracks to a common vertex, and require the χ^2 probability to exceed 0.1%.

The photon candidates used to reconstruct π^0 candidates are required to have a minimum laboratory energy of 100 MeV. The invariant masses of the candidate photon pairs are required to be within [0.1, 0.16] GeV/ c^2 . The masses of π^0 candidates are then constrained to the world average value [13].

The ρ^\pm candidates are formed by combining a π^\pm candidate with a π^0 candidate. The production angle θ^* is defined as the angle between the ρ^+ meson direction and the incident e^- beam in the e^+e^- center-of-mass. The ρ^\pm helicity angles θ_\pm are defined as the angles in the ρ^\pm rest frame between the direction of the boost from the laboratory frame and the direction of the π^\pm . We require $|\cos\theta^*| < 0.8$ and $|\cos\theta_\pm| < 0.85$ because there is low signal efficiency outside this fiducial region.

Figure 1 shows the scatter plot of the invariant mass $m_{\pi^+\pi^0\pi^-\pi^0}$ versus the absolute momentum difference $|\Delta p|$ in the laboratory frame between the $\pi^+\pi^0\pi^-\pi^0$ and initial e^+e^- systems after requiring the $\pi^\pm\pi^0$ masses to be less than 1.5 GeV/ c^2 . The last requirement eliminates a twofold ambiguity in forming the ρ^\pm candidates. A few per cent of the events have more than one ρ^+ or ρ^- candidate because of multiple π^0 's. All candidates are kept.

We accept events from within the rectangular area indicated in Fig. 1 ($|m_{\pi^+\pi^0\pi^-\pi^0} - \sqrt{s}| < 0.28$ GeV/ c^2 and $|\Delta p| < 0.2$ GeV/ c). There are a total of 612 candidates from 571 events in the $\Upsilon(4S)$ and off-resonance samples combined. Figure 2 shows the scatter plot of the invariant masses of $\pi^+\pi^0$ and $\pi^-\pi^0$ pairs from the accepted candidates. The concentration of candidates in the $\rho^+\rho^-$ mass range indicates $\rho^+\rho^-$ production.

We use a two-dimensional maximum likelihood fit to extract the signal for $e^+e^- \rightarrow \rho^+\rho^-$. Since the final state particle masses are far below the e^+e^- collision energy, we treat the two-body masses as uncorrelated. The signal probability density function (PDF) is constructed as a product of two identical one-dimensional PDFs for ρ^+ and ρ^- . We use a P -wave relativistic Breit-Wigner for-

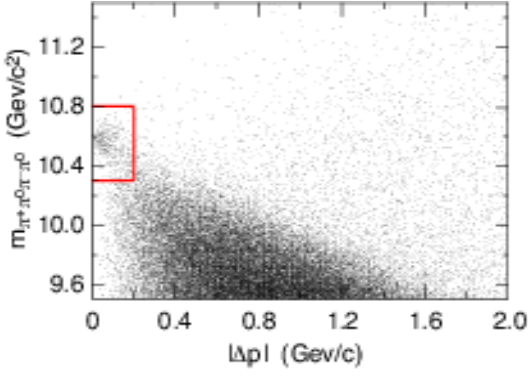


FIG. 1: Scatter plot of $m_{\pi^+\pi^0\pi^-\pi^0}$ vs. $|\Delta p|$ between the $\pi^+\pi^0\pi^-\pi^0$ and initial e^+e^- systems for the on-resonance data.

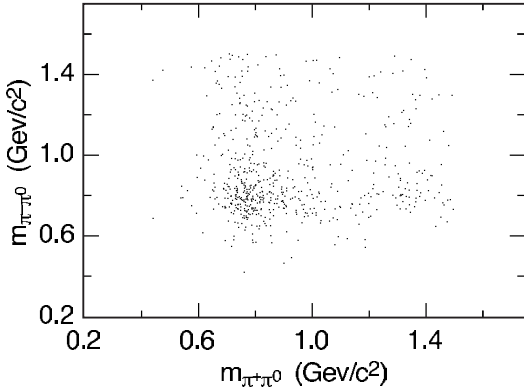


FIG. 2: Scatter plot of $m_{\pi^+\pi^0}$ and $m_{\pi^-\pi^0}$ for the accepted events in the combined data.

mula to construct the PDF for the ρ^\pm resonance:

$$F(m) \propto \frac{m\Gamma(m)}{(m_0^2 - m^2)^2 + m_0^2\Gamma^2(m)}, \quad (1)$$

$$\Gamma(m) = \Gamma_0 \left(\frac{q}{q_0}\right)^3 \left(\frac{m_0}{m}\right) \left(\frac{1 + q_0^2 R^2}{1 + q^2 R^2}\right),$$

where m is the observed pion-pair mass, Γ is the mass-dependent ρ width, and q is the absolute value of the pion candidate momentum in the ρ candidate rest frame. The 0 subscript indicates the value at the central mass of the ρ resonance. R is the Blatt-Weisskopf damping radius, which we set to $3 \text{ (GeV}/c)^{-1}$ [14, 15].

A threshold function $q^3/(1 + q^3\alpha)$ is used to model the background in the $\rho^\mp\pi^\pm\pi^0$ system, where α is a shape parameter. We use a linear function to model the residual two-dimensional background:

$$B(m_{\pi^+\pi^0}, m_{\pi^-\pi^0}) = 1 + a(m_{\pi^+\pi^0} - M) + a(m_{\pi^-\pi^0} - M), \quad (2)$$

where a is a floating parameter, and $M = 0.89 \text{ GeV}/c^2$ is the midpoint of the $\pi^\pm\pi^0$ invariant mass range used in the fit.

In the fit to the data, we fix the mass and width of the ρ^\pm to the world average values [13]. The parameters varied in the fit are: α [$\alpha(\pi^+\pi^0) = \alpha(\pi^-\pi^0)$], a , and the numbers of events for the four components: $\rho^+\rho^-$, $\rho^+\pi^-\pi^0$, $\rho^-\pi^+\pi^0$, and the residual background. The mass projections on $m_{\pi^+\pi^0}$ and $m_{\pi^-\pi^0}$ from the two-dimensional fit are shown in Fig. 3. The extracted number of $\rho^+\rho^-$ signal events is 357 ± 29 , with 329 ± 25 in the $\Upsilon(4S)$ resonance sample and 31 ± 14 in the off-resonance sample.

Assuming that the $\rho^+\rho^-$ is produced through a $J^{PC} = 1^{--}$ object (a single-photon or $\Upsilon(4S)$), and that C and parity P are conserved, there are three independent complex helicity amplitudes, F_{00} , F_{10} , and F_{11} , where the indices indicate the helicities of the ρ mesons. $F_{10} = F_{\pm 10} = F_{0\pm 1}$, $F_{11} = F_{-1-1}$, and $F_{1-1} = F_{-11} = 0$ due to angular momentum conservation [16]. The angular distribution of $\rho^+\rho^-$ decay products can be expressed as:

$$\begin{aligned} \frac{dN}{d \cos \theta^* d \cos \theta_+ d \varphi_+ d \cos \theta_- d \varphi_-} &\propto |A_{+1}|^2 + |A_{-1}|^2, \\ A_{\pm 1} &= \sin \theta^* \cos \theta_+ \cos \theta_- |F_{00}| \\ &\quad + \sin \theta^* \sin \theta_+ \sin \theta_- \cos(\varphi_+ + \varphi_-) |F_{11}| e^{i\varphi_{11}} \\ &\quad + \frac{1}{2} \sin \theta_+ \cos \theta_- (\pm(1 \mp \cos \theta^*)) e^{i\varphi_+} \\ &\quad \mp (1 \pm \cos \theta^*) e^{-i\varphi_+} |F_{10}| e^{i\varphi_{10}} \\ &\quad + \frac{1}{2} \cos \theta_+ \sin \theta_- (\pm(1 \mp \cos \theta^*)) e^{i\varphi_-} \\ &\quad \mp (1 \pm \cos \theta^*) e^{-i\varphi_-} |F_{10}| e^{i\varphi_{10}}, \end{aligned} \quad (3)$$

where φ_\pm is the azimuthal angle that corresponds to the helicity (polar) angle θ_\pm defined above. In this coordinate system, the incoming electron direction has an azimuthal angle φ_\pm of zero. The angles φ_{11} and φ_{10} are the strong phases of the amplitudes. Due to limited statistics, we examine only the projections and thus lose sensitivity to these phases.

The one-dimensional angular distributions are obtained from Eq. (3) by integrating over all other angles. When integrating over the full angular range, the results are

$$\begin{aligned} \frac{dN}{d \cos \theta^*} &\propto \sin^2 \theta^* |F_{00}|^2 \\ &\quad + f_1 (1 + \cos^2 \theta^*) |F_{10}|^2 + f_2 \sin^2 \theta^* |F_{11}|^2, \end{aligned} \quad (4)$$

$$\begin{aligned} \frac{dN}{d \cos \theta_\pm} &\propto \cos^2 \theta_\pm |F_{00}|^2 \\ &\quad + (f_3 + f_4 \cos^2 \theta_\pm) |F_{10}|^2 + f_5 \sin^2 \theta_\pm |F_{11}|^2, \end{aligned} \quad (5)$$

$$\frac{dN}{d \varphi_\pm} \propto |F_{00}|^2 + (f_6 - f_7 \cos 2\varphi_\pm) |F_{10}|^2 + f_2 |F_{11}|^2, \quad (6)$$

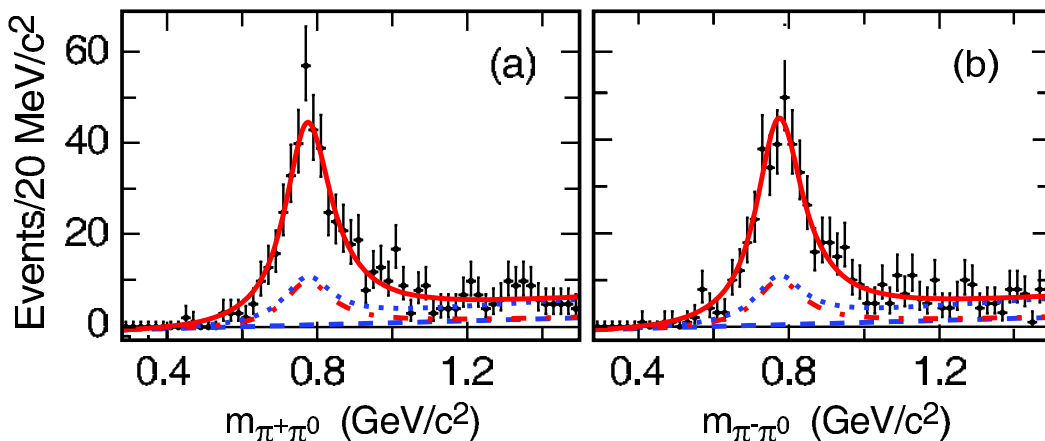


FIG. 3: The invariant mass projections a) $m_{\pi^+\pi^0}$ ($m_{\pi^-\pi^0} < 1.5$ GeV/ c^2) and b) $m_{\pi^-\pi^0}$ ($m_{\pi^+\pi^0} < 1.5$ GeV/ c^2) for accepted events in the combined data. The blue-dashed line is the residual linear background, the red dot-dashed line adds a) $\rho^+\pi^-\pi^0$, b) $\rho^-\pi^+\pi^0$, and the blue-dotted line includes both $\rho^+\pi^-\pi^0$ and $\rho^-\pi^+\pi^0$. The red solid line adds the signal.

where the constants f_n are given in the first row of Table I.

TABLE I: Constants in equations 4, 5, and 6.

Integrated region	f_1	f_2	f_3	f_4	f_5	f_6	f_7
Full range	2	2	1	1	1	4	1
Fiducial region	3.15	4.97	0.77	1.66	1.58	6.44	3.15

To determine the amplitude factors, we perform fits of Eqs. 4, 5, and 6 to the data. The fits are performed in the fiducial region $|\cos\theta^*| < 0.8$ and $|\cos\theta_{\pm}| < 0.85$. Limiting the integration to this fiducial region yields the constants shown in the second row of the table.

We use the sPlot [17] technique to subtract backgrounds in the measured angular distributions. This technique assigns a weight to each event (sWeight) for each category to which it might belong. The sWeights are obtained from the 2D fit to the $m_{\pi^-\pi^0}$ versus $m_{\pi^+\pi^0}$ distribution. We subdivide $\cos\theta^*$ and $\cos\theta_{\pm}$ into bins and produce an efficiency table from a phase-space-based Monte Carlo (MC) simulation. The event weight is given by the sWeight divided by the efficiency.

The background-subtracted and efficiency-corrected distributions for $\cos\theta^*$, φ_{\pm} , and $\cos\theta_{\pm}$ are shown in Fig. 4. We perform a simultaneous fit of Eqs. 4, 5, and 6 to the five angular distributions, assuming there are no correlations between the variables. We return to the issue of correlations when we discuss systematic uncertainties. In the fit, the amplitudes are constrained to satisfy $|F_{00}|^2 + 4|F_{10}|^2 + 2|F_{11}|^2 = 1$, since there are one F_{00} , four F_{10} and two F_{11} amplitude components. The free parameters in the fit are $|F_{00}|^2$, $|F_{10}|^2$ and the overall normalization. The value and error of $|F_{11}|^2$ is

derived from the fit result and its full covariance matrix using $F_{11} = \frac{1}{2}(1 - |F_{00}|^2 - 4|F_{10}|^2)$. The normalized amplitudes are: $|F_{00}|^2 : |F_{10}|^2 : |F_{11}|^2 = 0.51 \pm 0.14(\text{stat}) \pm 0.07(\text{syst}) : 0.10 \pm 0.04(\text{stat}) \pm 0.01(\text{syst}) : 0.04 \pm 0.03(\text{stat}) \pm 0.01(\text{syst})$.

To determine the significance of the result and the systematic errors in the fitting procedure, we performed fits to multiple sets of events generated according to Eq. 3 (toy MC). These studies allow us to assess biases that arise because of correlations. We find the biases in the fitted ratios of squared moduli to be less than 0.002, which are included in the systematic errors. Most of these biases are due to the imperfect MC efficiency corrections that result from the coarse bin size of the efficiency table. The statistical uncertainties are scaled using the RMS of the pull distributions from the toy MC study. The fitter underestimates the statistical uncertainties by approximately 6%. Other sources of systematic error, such as some of those described below for the cross section, have little dependence on angle, and thus are expected to be relatively small. We neglect them.

The measured value of $|F_{00}|^2$ deviates from 1.0, the value predicted by QCD models [6]. From the toy MC studies, we determine the statistical probability for this deviation to be less than 1 in 3000 experiments, corresponding to 3.4 standard deviations. Including systematic uncertainties, the significance is 3.1 standard deviations. This suggests that the production may not be dominated by single-photon annihilation as naively expected.

The cross section, including radiative corrections, for $e^+e^- \rightarrow \rho^+\rho^-$ is calculated from

$$\sigma = \frac{N}{\mathcal{L} \times \varepsilon \times (1 + \delta)}, \quad (7)$$

where N is the number of $\rho^+\rho^-$ signal events extracted

from the combined data, \mathcal{L} is the integrated luminosity, and ε is the signal efficiency obtained from MC simulation that uses the fully differential angular distribution derived from the results of the form factor fit. The $\rho^+\rho^-$ signal efficiency in the fiducial region, without radiative corrections, is estimated to be 15.0%. The correction for initial state radiation, $1 + \delta$, is calculated according to Ref. [18] and has the value 0.775. Assuming single-photon production, the radiatively corrected cross section near $\sqrt{s} = 10.58$ GeV for $m_{\rho^\pm} < 1.5$ GeV/ c^2 and within $|\cos\theta^*| < 0.8$, $|\cos\theta_\pm| < 0.85$ is $8.3 \pm 0.7(\text{stat}) \pm 0.8(\text{syst})$ fb. Using Eq. 3, we can scale the cross section from our acceptance to the full angular ranges, which gives $19.5 \pm 1.6(\text{stat}) \pm 3.2(\text{syst})$ fb, where the systematic error includes ± 1.7 fb due to the effect of the uncertainties in the amplitudes on the extrapolation.

To study the possibility that the observed signal arises from $\Upsilon(4S) \rightarrow \rho^+\rho^-$ decay, we scale the off-resonance signal to the on-resonance luminosity, and subtract it from the on-resonance signal. The resulting number of events, 35 ± 135 , is consistent with zero. The corresponding branching fraction for $\Upsilon(4S) \rightarrow \rho^+\rho^-$ is $(8.1 \pm 29.0) \times 10^{-7}$. The systematic errors, which may be estimated from those given below for the cross section, are negligible for this branching fraction measurement. Restricting possible results to the physical region (≥ 0), the Bayesian 90% confidence level upper limit is 5.7×10^{-6} .

The systematic uncertainty on the $e^+e^- \rightarrow \rho^+\rho^-$ cross section, due to uncertainties in the angular distribution fit, is estimated by varying the amplitude values. The systematic uncertainty from the two-dimensional fit is estimated from the difference in yield obtained by allowing the mean and width of the ρ resonance mass to vary in the fit. The systematic uncertainties due to π^\pm identification, tracking, and π^0 efficiency are estimated based on measurements from control data samples. The possible background from related modes with extra particles is estimated by using extrapolations from four-particle mass sidebands. The systematic uncertainties are summarized in Table II.

TABLE II: Systematic uncertainties on the fiducial region cross section of $e^+e^- \rightarrow \rho^+\rho^-$.

Source	Systematic uncertainty %
Amplitude fit	5.2
Two-dimensional fit	2.0
Particle Identification	2.3
Tracking efficiency	1.0
π^0 efficiency	6.0
$\rho^+\rho^- + X$ feed-down	4.9
Luminosity	2.0
Radiative corrections	1.0
Total	10.0

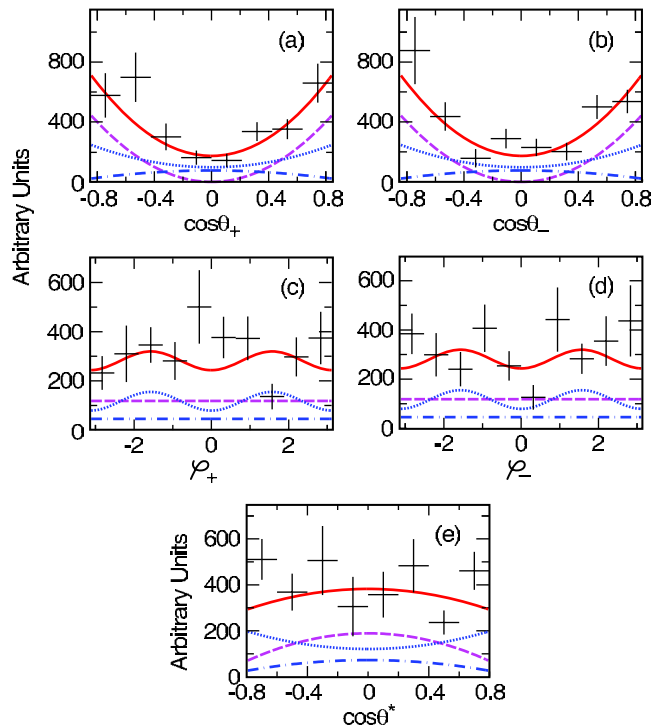


FIG. 4: The background-subtracted (sWeighted) and efficiency-corrected a) $\cos\theta_+$ b) $\cos\theta_-$ c) φ_+ d) φ_- and e) $\cos\theta^*$ distributions. The magenta dashed line is the contribution from the F_{00} component, the blue dotted line is for the F_{10} component, the blue dot-dashed line is for the F_{11} component, and the red solid line is the total fit function.

In summary, we have presented the first observation of the exclusive production of $\rho^+\rho^-$ in e^+e^- interactions near $\sqrt{s} = 10.58$ GeV and measured the relative amplitudes of the three helicity components. Assuming production through single-photon annihilation, the cross section is measured to be $\sigma(e^+e^- \rightarrow \rho^+\rho^-) = 19.5 \pm 1.6(\text{stat}) \pm 3.2(\text{syst})$ fb. The 90% confidence level upper limit on the branching fraction $\mathcal{B}(\Upsilon(4S) \rightarrow \rho^+\rho^-)$ is 5.7×10^{-6} . Our result for the $|F_{00}|^2$ amplitude is inconsistent by 3.1 standard deviations with the predictions of QCD models that assume single-photon production, however, indicating that other mechanisms such as TVPA with FSI may be important.

We are grateful for the excellent luminosity and machine conditions provided by our PEP-II colleagues, and for the substantial dedicated effort from the computing organizations that support *BABAR*. We wish to thank S. Brodsky, A. Goldhaber, and L. Dixon for helpful discussions. The collaborating institutions wish to thank SLAC for its support and kind hospitality. This work is supported by DOE and NSF (USA), NSERC (Canada), CEA and CNRS-IN2P3 (France), BMBF and DFG (Germany), INFN (Italy), FOM (The Netherlands), NFR (Norway), MES (Russia), MEC (Spain), and STFC

(United Kingdom). Individuals have received support from the Marie Curie EIF (European Union) and the A. P. Sloan Foundation.

* Deceased

† Now at Temple University, Philadelphia, Pennsylvania 19122, USA

‡ Now at Tel Aviv University, Tel Aviv, 69978, Israel

§ Also with Università di Perugia, Dipartimento di Fisica, Perugia, Italy

¶ Also with Università di Roma La Sapienza, I-00185 Roma, Italy

** Now at University of South Alabama, Mobile, Alabama 36688, USA

†† Also with Università di Sassari, Sassari, Italy

- [1] K. Abe *et al.* (Belle Collaboration), Phys. Rev. Lett. **89**, 142001 (2002); K. Abe *et al.* (Belle Collaboration), Phys. Rev. D **70**, 071102 (2004).
- [2] B. Aubert *et al.* (BABAR Collaboration), Phys. Rev. D **72**, 031101 (2005).
- [3] E. Braaten and J. Lee, Phys. Rev. D **67**, 054007 (2003), [Erratum-ibid. D **72**, 099901 (2005)]; K. Y. Liu, Z. G. He and K. T. Chao, Phys. Lett. B **557**, 45 (2003).
- [4] A. E. Bondar and V. L. Chernyak, Phys. Lett. B **612**, 215 (2005); G. T. Bodwin, D. Kang and J. Lee, Phys. Rev. D **74**, 114028 (2006); Y. Zhang, Y. Gao, and K. T. Chao, Phys. Rev. Lett. **96**, 092001 (2006); G. T. Bodwin, D. Kang, T. Kim, J. Lee, and C. Yu, AIP Conf. Proc. **892**, 315 (2007); G. T. Bodwin, J. Lee, and C. Yu, Phys. Rev. D **77**, 094018 (2008).
- [5] B. Aubert *et al.* (BABAR Collaboration), Phys. Rev. D **74**, 111103(R) (2006).
- [6] G. P. Lepage and S. J. Brodsky, Phys. Rev. D **22**, 2157 (1980); S. J. Brodsky and G. P. Lepage, Phys. Rev. D **24**, 2848 (1981); V. Chernyak, arXiv:hep-ph/9906387; V. L. Chernyak and A. R. Zhitnitsky, Phys. Rept. **112**, 173 (1984).
- [7] B. Aubert *et al.* (BABAR Collaboration), Phys. Rev. Lett. **97**, 112002 (2006).
- [8] M. Davier, M. Peskin, and A. Snyder, arXiv:hep-ph/0606155.
- [9] G. T. Bodwin, E. Braaten, J. Lee and C. Yu, Phys. Rev. D **74**, 074014 (2006).
- [10] M. Gell-Mann, D. Sharp, and W. G. Wagner, Phys. Rev. Lett. **8**, 261 (1962); M. Diehl, P. Kroll, and C. Vogt, Phys. Lett. B **532**, 99-110 (2002).
- [11] A. B. Kaidalov and M. I. Vysotsky, Phys. Lett. B **652**, 203 (2007). A. Datta *et al.*, Phys. Rev. D **76**, 034015 (2007).
- [12] B. Aubert *et al.* (BABAR Collaboration), Nucl. Instrum. Meth. Phys. Res., Sect. A **479**, 1 (2002).
- [13] W. M. Yao *et al.* [Particle Data Group], J. Phys. G **33**, 1 (2006).
- [14] D. Aston *et al.*, Nucl. Phys. B **296**, 493 (1988).
- [15] S. Godfrey and N. Isgur, Phys. Rev. D **32**, 189 (1985).
- [16] M. Jacob, and G. C. Wick, Ann. Phys. **7**, 404 (1959); S. U. Chung, Phys. Rev. D **57**, 431 (1998).
- [17] M. Pivk and F. R. Le Diberder, Nucl. Instrum. Meth. Phys. Res., Sect. A **555**, 356 (2005).
- [18] M. Benayoun, S. I. Eidelman, V. N. Ivanchenko and Z. K. Silagadze, Mod. Phys. Lett. A **14**, 2605 (1999).